International Journal of Thermal Sciences 204 (2024) 109244

Contents lists available at ScienceDirect

International Journal of Thermal Sciences

journal homepage: www.elsevier.com/locate/ijts

Assessment of nozzle performance in high-viscosity oil spray system for rectangular copper conductors☆,☆☆

Payam Shams Ghahfarokhi [a,*], Andrejs Podgornovs [b], Antonio J. Marques Cardoso [c], Paavo Rasilo [a]

[a] Electrical Engineering Unit, Tampere University, P.O.Box 692, FI-33014, Finland
[b] Department of Electrical Machines and Apparatus, Riga Technical University, Riga, Latvia
[c] CISE - Electromechatronic Systems Research Centre, University of Beira Interior, Portugal

ARTICLE INFO

Keywords:
Direct oil spray cooling
Heat transfer coefficient
High viscosity
Nozzle
Temperature measurement
Thermal management system

ABSTRACT

This article presents a detailed examination of the performance characteristics of a high-viscosity spray oil cooling system, utilizing various commercial nozzles. These include one spiral hollow cone nozzle, three full cone nozzles, and three flat fan nozzles, all of which were subjected to experimental investigation. Parameters such as temperature, temperature uniformity, injection pressure, spray coverage, spray patterns, spray angles, spray capacitance, heat transfer coefficient, and spray power consumption were assessed to gauge the system's effectiveness. To conduct these experiments, a dedicated test bench was constructed, and a range of commercial nozzles with different spray patterns (full cone, hollow cone, and flat fan) and spray angles (narrow, medium, and wide) were selected. Through a series of experiments, the influence of various nozzle input parameters was scrutinized, with a focus on heat transfer capabilities, temperature uniformity, and cooling efficiency. The results revealed that increasing the nozzle's inlet pressure significantly improves its performance. Moreover, nozzles with medium to wide spray angles demonstrated the best cooling performance, particularly flat fan nozzles in this category. Based on these findings, the article offers recommendations to enhance temperature regulation and cooling efficiency for improved overall system performance.

1. Introduction

In the recent decade, the globe has faced a trend in transportation electrification, including all transportation types - maritime, aerospace, railways, and roads - to moderate the negative impact of combustion engines on greenhouse gases and global warming. The research studies present the different growth and maturity development steps for various transportation types. One of the main aspects of this global tendency is manufacturing a new generation of electric machines with high power density, compact size, cost-effectiveness, and lightweight structure [1,2]. One of the practical options to achieve the aforementioned goals for electric motors, especially for electric vehicle (EV) motors, is replacing the conventional round winding with hairpin windings [3,4]. These novel windings offer various advantages, such as increasing the current density, a high slot-filling factor, and lower manufacturing time and cost [5–8]. Besides, they have geometrical advantages through defined accurate positioning of the rectangular conductors and precise gaps among the end winding parts of the hairpin configuration [9].

Parallel to developing new electromagnetic designs for electric motors, it is essential to develop advanced thermal management systems to augment their power density, heat extraction, and reliable operation. One of the potential thermal management systems matching the new generation of EV motors with the hairpin windings is the oil spray cooling system. The main idea behind this cooling system is to reduce the thermal path from the windings as the main heat loss source to the cooling system and use the geometrical advantages of the hairpin windings. By implementing this cooling system, the oil is directly in contact with the end winding, which provides enormous axial heat transfer in the slot.

There are many research studies considering the spray cooling system [10–16]; however, most of them investigated the implementation of a spray cooling system on thermal engineering devices with coolants

☆ This paper has not been presented at any conferences and has not been submitted elsewhere.☆☆ This work was supported by the Academy Research Fellow granted by the Research Council of Finland with decision No. 355019 and CoE 346440.

* Corresponding author.
E-mail address: payam.shamsghahfarokhi@tuni.fi (P. Shams Ghahfarokhi).

https://doi.org/10.1016/j.ijthermalsci.2024.109244
Received 10 May 2024; Received in revised form 3 June 2024; Accepted 28 June 2024
Available online 2 July 2024

such as water, evaporators, and refrigerants. Their findings and conclusions are not relevant and applicable to windings of electrical machines.

Recently, the number of research studies has increased with the increasing popularity of utilizing oil spray cooling systems for hairpin windings. Liu et al. [9,17,18] presented one of the early studies on integrating the oil spray cooling system with an electric motor with hairpin windings. In the first step, they experimentally investigated the cooling performance of oil spray setups on the end parts of hairpin configuration by comparing heat transfer coefficient (HTC) and winding temperature during various flow rates, pressures, and nozzle outlet velocities. Finally, they developed the reduced parameter models to estimate the HTC of the spray cooling system mounted axially and radially on the end parts of the hairpin windings. However, the results only consider two different types of nozzles, and the correlation was only developed based on the performance of the full-cone nozzle.

Zhang et al. [19] proposed a 3-D analytical thermal analysis approach for oil spray cooled hairpin windings, which was able to model the uneven temperature distribution in the end windings caused by the nonuniform oil spray distribution by the nozzles. However, their model only considered the stator, and no information was provided about the impact of the rotor and rotational speed on the motor's heat transfer and thermal model.

Gronwald et al. [20] developed a transient thermal model for the oil spray-cooled hairpin winding to model and determine the HTC from the end winding using empirical correlations based on dimensionless numbers. However, they considered a single flat jet nozzle.

The aforementioned studies show the potential of the spray system to cool electric machines with hairpin windings. They demonstrate different maturity levels for this concept, implying that the technology is still in progress of becoming feasible in practice. Further research is thus required in the cooling method, system development, and analysis approaches.

At the beginning of the authors' research on spray cooling systems, they presented in Ref. [21] a summary of attempts to implement the spray cooling system on electrical machines and a review of the evolution of this cooling system over the years. Based on the findings, the main issues of the oil spray cooling system on electrical machines are divided into three categories:

1. high viscosity of coolant
2. uneven temperature distribution in the end winding
3. lack of systematic analysis and design methodology.

Regarding the first and second issues, the authors have experimentally investigated in Ref. [22] the impact of high viscosity on the spray cooling system performance, particularly on the nozzle's performance and on nonuniform temperature distribution. From the systematic analysis and design methodology, there is little experimental data related to the performances of various nozzles, their spray coverage, and the impact of input parameters of nozzles on their performances with oil as a high-viscosity coolant. This article's contribution lies in its experimental exploration of nozzles' performance and a comprehensive analysis of various parameters affecting nozzle efficiency and heat transfer. The ultimate goal is to contribute to the development of a systematic analysis and design methodology in this domain.

2. Experimental setup and procedure

The idea of this study is to experimentally consider the performance of various nozzles and the impact of their input parameters (inlet pressure and flow rate) on heat transfer and temperature uniformity. For this purpose, at the beginning of this section, the design and construction of the hydraulic setup are explained in detail. Next, the nozzles under investigation and their characteristics are introduced. Then, the data collection and test procedure are discussed. Finally, the data processing for assessing the operation of the spray system with various nozzles is described.

A. Test Bench Design

As seen in Fig. 1, the setup is divided into two main sections: the hydraulic system and the spray cooling section. The hydraulic system is a closed-loop system responsible for circulating the oil as a coolant. This system includes several components: coolant, pump, valve, tank, and temperature unit. In this system, the pump boosts the oil pressure from the tank to the spray cooling section, and the valve can adjust the system's pressure. A frequency converter controls the rotational speed of the pump motor to adjust the flow rate. The nozzle in the spray cooling section alters the liquid into tiny droplets and sprays it on the hairpin conductor. After the oil is sprayed onto the hairpin conductor, it is gathered from the outlet port of the spray cooling section by gravity and sent back to the oil temperature unit to prepare for recirculation.

As seen in Fig. 1 b), the spray cooling section includes a housing, a nozzle, a rectangular conductor, conductor holders, inlet and outlet ports, and adjustable elevators that enable the holders to be mounted at desirable heights. The housing with the dimensions of 300 mm $\times$ 300 mm $\times$ 132 mm consists of two parts: casing and transparent cover (Fig. 2). The casing (as the housing base) is made of fiberglass-reinforced polycarbonate, and the transparent cover is made of acrylic plexiglass.

Moreover, the conductor holders and adjustable elevators are made of PLA filament using additive manufacturing techniques. As seen in Fig. 2, all the mentioned devices are fitted inside the casing, and the transparent cover coats the housing to prevent oil leakage. The nozzle is fixed vertically inside the nozzle port located in the middle of the housing's top side, and the sprayed oil is collected from the downside of the housing from the outlet port.

The oil as coolant utilized in the experiment is a fully synthetic lubricant whose detailed properties are given in Table I. Two filters are added to the input and output of the system to prevent the nozzle and fluid system from clogging and blockage.

The hairpin conductor has a large cross-section with low resistance. Therefore, the system requires a high current to generate adequate copper losses for heating the conductor. For this purpose, one microwave transformer with welding wire as the secondary winding was used to reach the current to 110 A in the conductor.

B. Nozzles

Nozzles are the mechanical apparatus that convert the liquid flow to droplets. The process of altering the fluid flow into tiny droplets is called atomization. The atomization process can occur by two main factors: fluid flow pressure or a mixture of air and fluid [21]. As a result, the nozzles can be categorized into two main groups: hydraulic nozzles and two-fluid (air-assisted) nozzles [23,24].

However, hydraulic nozzles are preferable for the oil spray-cooling system of electric motors due to their reliance on liquid momentum to generate droplets. Besides, hydraulic nozzles provide a more straightforward hydraulic system than two-fluid nozzles by not using a non-condensable gas and a liquid coolant for the atomization process, which leads to no requirement of segregating the gas from the liquid coolant since the segregation system of gas from liquid significantly enhances the cooling system's complexity [23]. Therefore, this paper investigates hydraulic nozzles with various spray patterns: flat fan, full cone, and hollow cone. Table II presents the details of the nozzles' parameters used in the study. According to the data presented in Table 2, the full cone and hollow cone nozzles are low flow rate nozzles, and flat fan nozzles are high flow rate ones. Fig. 3 illustrates the spray patterns of the nozzles under study and the distance of the nozzles from the rectangular conductor.

C. Monitoring Instruments and Data Collection

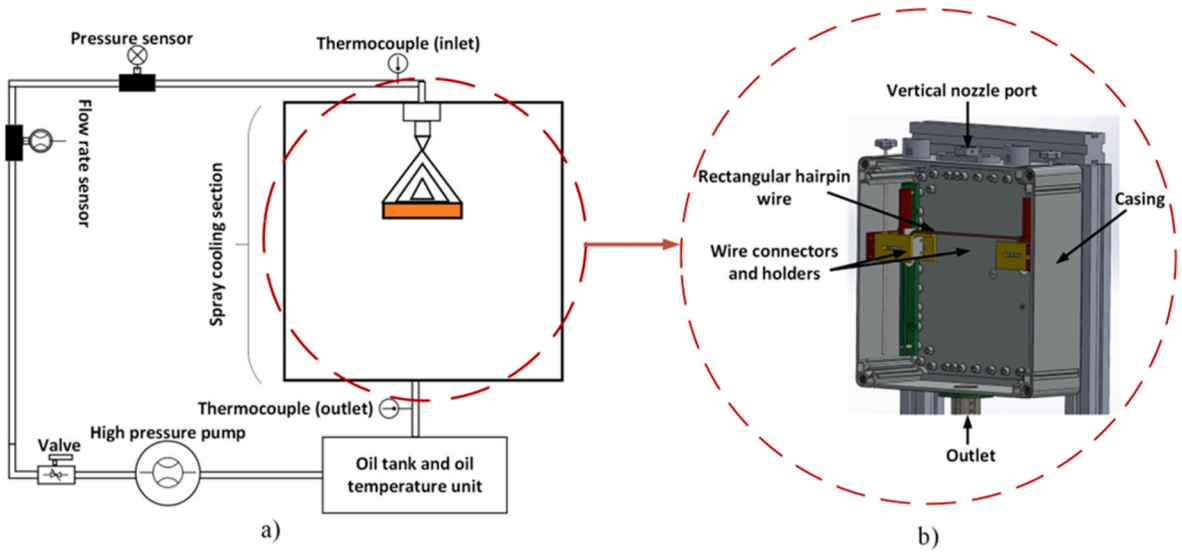

Fig. 1. Test bench schematic. a) The hydraulic system. b) The spray cooling section.

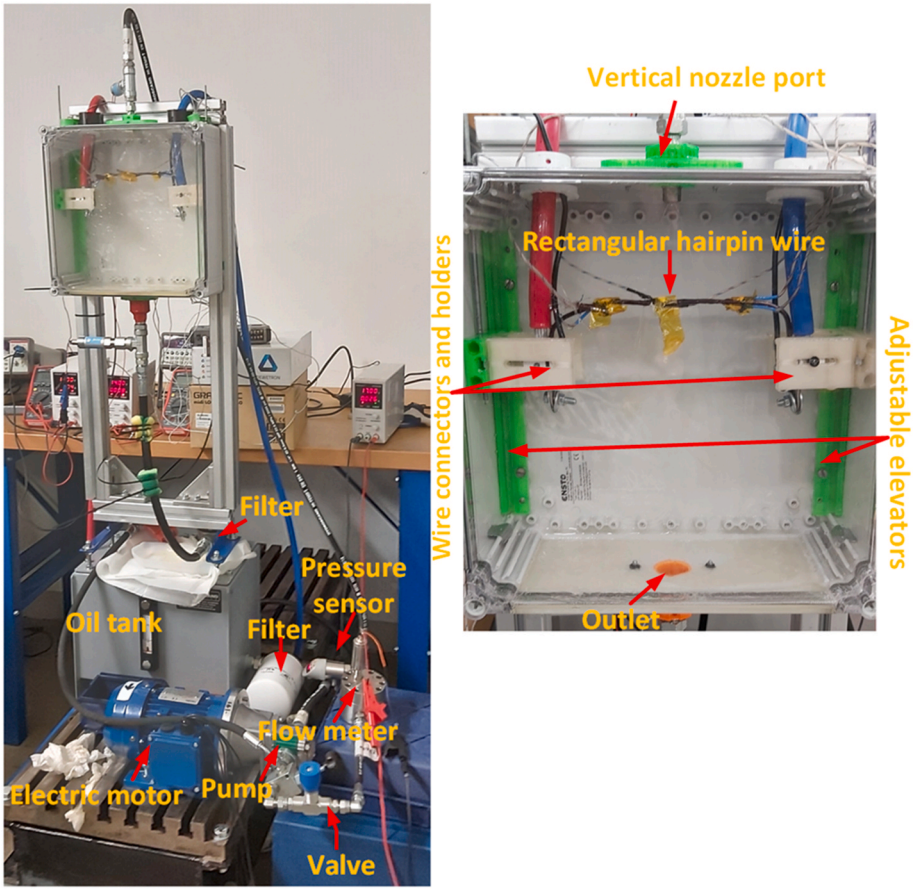

Fig. 2. Test setup.

Table 1
Material properties of oil.

Property	Value
Viscosity at 40 °C	1×10^{-5} m^2/s
Viscosity at 100 °C	2.7×10^{-6} m^2/s
Density at 15 °C	0.84 kg/m^3

Several sensors and measurement devices were mounted on the system to evaluate and investigate the performance of various nozzles and the impact of the nozzle's inlet parameters (pressure, flow rate, coolant temperature) on the heat transfer and temperature distribution of the hairpin conductor. As seen in Fig. 1 a), a pressure transducer was installed in the hydraulic system to measure the flow pressure, and the oil flow rate was measured by the positive displacement meter (GF025-

Table 2
The nozzles' properties.

Nozzle type	Nozzle index	Spray angle (θ)	Flow rate (l/min)	Pressure (bar)	Orifice diameter (mm)
Flat fan	NF0365	65°	0.48–3.74	0.5–30	1.09
	NF0390	90°	0.48–3.74		1.09
	NF05120	120°	0.81–6.24		1.45
Hollow cone	L40	90°	0.53–1.69	0.7–7	1.02
Full cone	MPL0.3 N	53°	0.63–1.7	0.7–6	1.1
	MPL0.3 M	86°			0.99
	MPL0.3 W	134°			1.1

MAP-B-6). This type of flow meter handles working with high-viscosity fluid and can accurately measure the small flow rate. Besides, the inlet and outlet oil temperatures were measured using the TP125 series temperature sensors. As shown in Fig. 3, a total of six K-type thermocouples (T1-T6) were mounted using adhesive material to monitor the temperature distribution on the hairpin conductor. T1 and T2 were mounted at the extreme left side of the hairpin, at its upper and lower sides, respectively. T3 and T4 were installed in the middle of the hairpin conductor on the upper and lower sides. Finally, T5 and T6 were installed at the extreme right side of the rectangular conductor on its upper and lower sides, respectively.

The Digital Dual Measurement Multimeter (GDM-8342) and Clamp Multimeter (AMP 220) measured the AC voltage, current, and phase angle applied to the hairpin conductor, respectively. The thermal sensors' outcomes during the experiment were collected by the data acquisition system (GL840-WV) with a 10-s interval and sent to the computer for further analysis.

D. Experimental Procedure and Data Processing

The experiment's main objective is to investigate the performance of nozzles under various inlet pressures. For this purpose, the operation of each nozzle during various inlet parameters was considered by investigating the following parameters:

- heat transfer capability
- temperature uniformity
- cooling efficiency.

The heat transfer capability of the nozzles is evaluated by determining the HTC from the experimental data, and the standard deviation of temperature determines the temperature uniformity of the target surface cooled during each nozzle operation. Ultimately, the cooling efficiency of the setup is defined by spray system conductance and pumping power.

In the first step, when the system reaches its thermal stability, which is defined by a <0.5 °C change in the temperature within 30 min, the total power losses P can be calculated by

$$P = UI\cos\varphi, \tag{1}$$

where U and I are the root-mean-squared voltage and current applied to the hairpin conductor, respectively, and φ is the phase difference, which is very close to zero due to the low inductance of the conductor.

Then, the HTC is calculated as

$$h_T = \frac{P}{A_c(T_{av} - T_{in})}, \tag{2}$$

where A_c is the rectangular conductor surface area, T_{av} is the average temperature of the conductor, approximated as the average of the six thermocouple measurements, and T_{in} is the oil inlet temperature.

To assess the ability of the nozzles and the spray setup to provide temperature uniformity on the surface of the hairpin conductor, the standard deviation of the surface temperature σ is calculated. This value is a measure of how dispersed data is in relation to the mean. A low standard deviation indicates that data points are clustered tightly around the mean, while a high standard deviation indicates that data points are more spread out. A standard deviation close to zero suggests that data points are very close to the mean, whereas a larger standard deviation indicates that data points are spread further away from the mean, and it is calculated as

$$\sigma = \sqrt{\sum_{i=1}^{n} \frac{(T_i - T_{av})^2}{n}}, \tag{3}$$

where n is the total number of thermocouples attached to the surface of

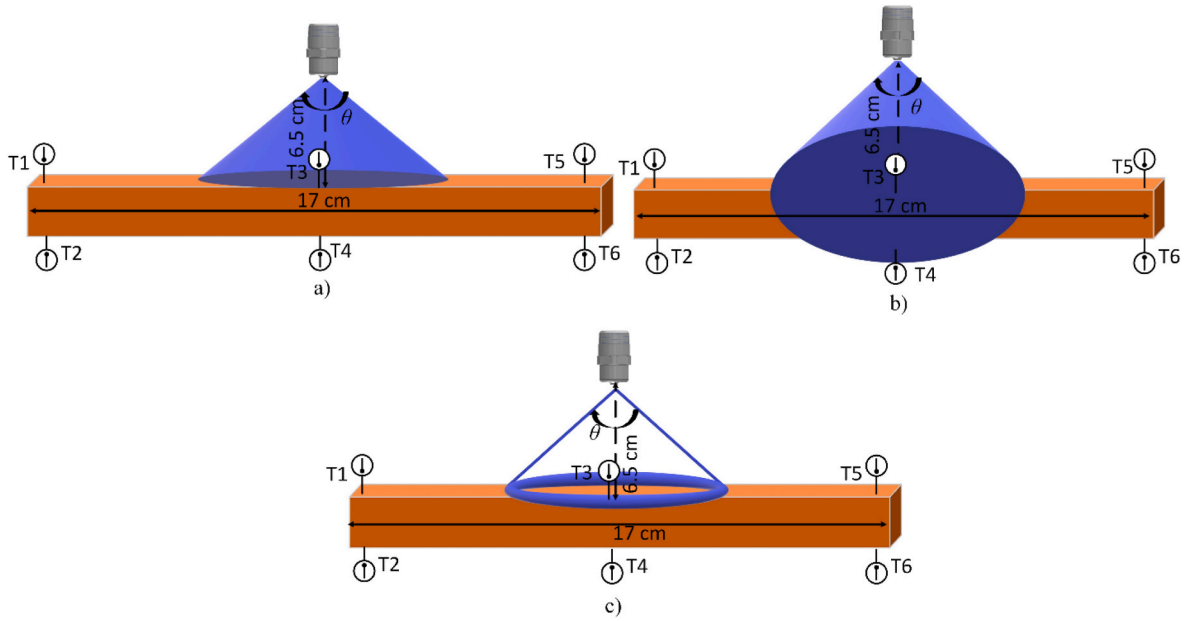

Fig. 3. Spray patterns of the nozzles under study with various spray angles θ. a) Spray pattern of flat fan nozzles. b) Spray pattern of full cone nozzles. c) Spray pattern of hollow cone nozzle.

the hairpin conductor, and T_i is the temperature of the ith thermocouple.

Ultimately, the cooling efficiency of the spray system with each nozzle is assessed by inlet pumping power P_p via thermal conductance C. For this purpose, these two parameters are evaluated, respectively, as:

$$P_p = p_{in}\dot{V}, \tag{4}$$

$$C = \frac{P}{T_{av} - T_{in}}, \tag{5}$$

where p_{in} is the nozzle's inlet pressure and $\dot{V}$ is the volumetric flow rate.

E. Uncertainty Analysis

The accuracy of the experimental data directly depends on the accuracy of the measurement equipment. Uncertainty analysis is an approach to finding the accuracy of the measurement data based on precision in the measurement equipment. The accuracies of the thermocouples, Digital Dual Measurement Multimeter and Clamp Multimeter, pressure transducer, and positive displacement meter are ±0.75 %, ±1 %, ±2.2 %, ±0.5 %, and ±0.5 %, respectively, In the first, the accuracy power loss (σ_P) is determined as:

$$\sigma_P = \pm\sqrt{\left(\frac{\partial P}{\partial V}\sigma_V\right)^2 + \left(\frac{\partial P}{\partial I}\sigma_I\right)^2} \tag{6}$$

where σ_V and σ_I are the voltage and current measurement accuracy, respectively.

Finally, the uncertainty value of the heat transfer coefficient is defined as:

$$\sigma_{hT} = \pm\sqrt{\left(\frac{\partial h_T}{\partial P}\sigma_P\right)^2 + \left(\frac{\partial h_T}{\partial T_{av}}\sigma_{Tav}\right)^2 + \left(\frac{\partial h_T}{\partial T_{in}}\sigma_{Tin}\right)^2} \tag{7}$$

where σ_{Tav} and σ_{Tin} are the uncertainty in the temperature measurement of the conductor surface and oil inlet. It should be noted the uncertainty analysis of HTC is evaluated as ±6.08 %, which means the measured value could vary by 6.08 % above or below the reported value.

3. Results

A series of experiments was carried out with different nozzles, and for each nozzle, the impact of inlet pressure and flow rate on the nozzle's operation was investigated. Moreover, the experimental data was collected for further analysis to investigate the nozzles' performances by determining the aforementioned parameters.

A. Nozzles' Inlet parameters

Fig. 4 shows the parametric behavior of the nozzles under investigation by illustrating the variation of their flow rate and outlet velocity versus various inlet pressures. However, the ranges of pressure and flow rate were limited due to the hydraulic system capability and spray system section. In this study, the outlet velocity of the nozzles was determined according to the total volumetric flow rate and the orifice area of the nozzles.

As seen in Fig. 4, the nozzles' flow rate and outlet velocity are pressure-dependent, and both parameters increase with increasing pressure. The hollow cone nozzle L40 has the lowest flow rate with high outlet velocities and medium spray angle. Unlike L40, the flat fan nozzle NF05120 has the highest flow rate and the lowest outlet velocity with a wide spray pattern. Other flat fan nozzles -NF0365 and NF0390- have almost similar flow rates and velocity performance with narrow and medium spray angles, respectively.

MPL0.3N–W as full cone nozzles almost provide the same flow rate ranges (same as NF0365) with different spray angles. However, from the nozzle's outlet velocity, the MPL0.3 M has the highest outlet velocity among all the nozzles, and MPL0.3 W, similar to NF05120, has the lowest nozzle's outlet velocity.

B. Heat Transfer Capability

The heat transfer capability of the spray system during the operation of various nozzles is investigated by comparing the HTC calculated with (1)-(2). Fig. 5 a), b), and c) show the variation of the HTC versus different parameters of the nozzles. As seen in these figures, by increasing the pressure, flow rate, and outlet velocity, the HTC

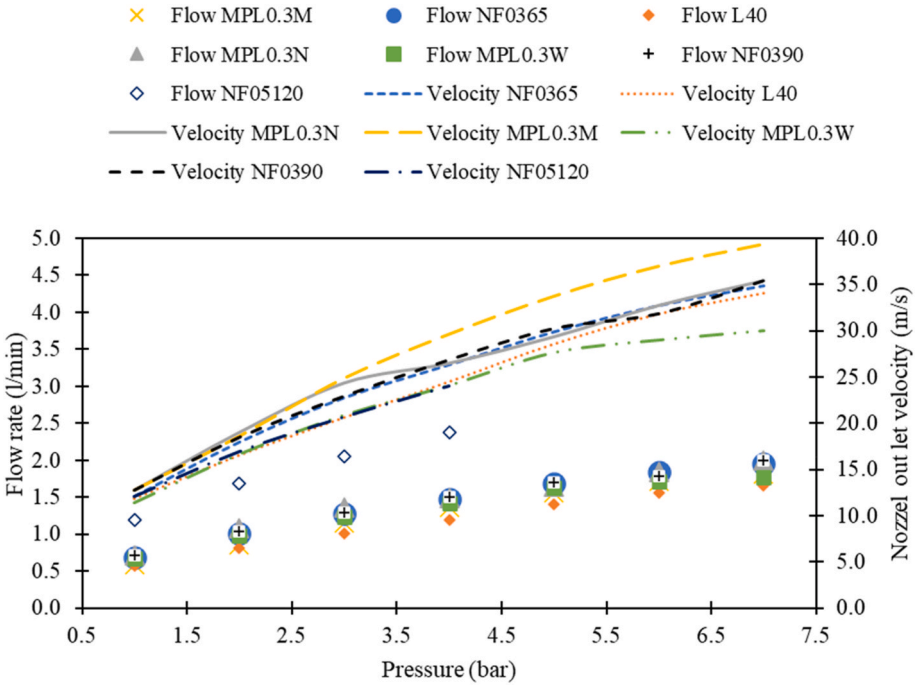

Fig. 4. The variation of the flow rate and outlet velocity of nozzles under investigation versus different inlet pressure.

increases, the increase being most significant for the flat fan and full cone nozzles. No significant changes were observed in the HTC of the hollow cone nozzle by changing the nozzles' pressure.

The two flat fan nozzles, NF0390 and NF05120, with medium and wide spray angles, respectively, demonstrate the best heat transfer capability in terms of the highest HTC. NF05120 provided the highest flow rate for a given pressure. Besides, more oil was sprayed onto the concentrated surface based on its spray pattern and coverage. A similar situation occurred for NF0390, but for the same pressure, the HTC of this nozzle is less than that of NF05120 due to the lower flow rate. Among the flat fan nozzles, the weakest heat transfer performance belongs to NF0365. This nozzle has a similar flow rate for a given pressure as NF0390, but due to the narrow spray pattern, it may not cover the entire surface of the rectangular conductor, leading to a higher average surface temperature and lower HTC.

In comparison to the flat fan nozzles, the full cone nozzles provided wider spray coverages and spray patterns, which led to less oil spraying onto the target surfaces. MPL0.3 M with medium spray angle performed best among the full cone nozzles. Moreover, this nozzle had the highest outlet velocity among all the nozzles.

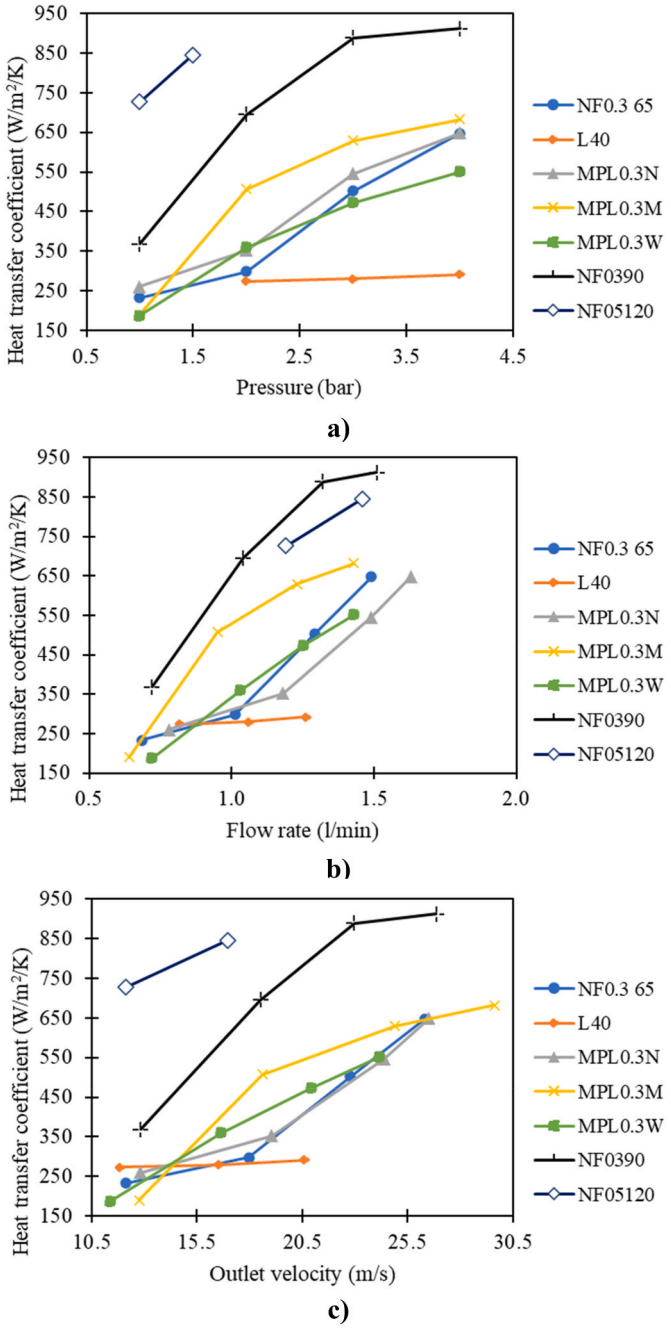

Fig. 5. HTC variation during various nozzles' parameters. a) Versus the nozzle's inlet pressure. b) Versus the nozzle's flow rate. c) Versus the nozzle's outlet velocity.

C. Temperature *Distribution and Uniformity*

One of the main challenges in using the oil spray cooling system is the uneven temperature distribution due to the non-uniform nozzle coverage. This uneven temperature distribution may lead to hotspots in the end windings of the machines, which may exceed the temperature limit of the winding insulation and cause a reduction in the lifetime of the electric motor and faults. Here in this section, the performance of nozzles from temperature rise and temperature uniformity point of view are investigated.

In the first step, the average temperature rise versus the nozzles' outlet velocity is considered. The average temperature rise is defined as the difference between the mean measured temperature of the rectangular conductor and the oil inlet temperature. Fig. 6 shows the variation of the average temperature rise of the hairpin conductor versus the nozzles' outlet velocity. As seen in the figure, the cooling performance improved by increasing the nozzle outlet velocity, and the temperature rise decreased due to the increase in the flow rate. By comparing data in Fig. 6, the flat fan nozzles with medium and large spray coverage (NF0390, NF05120) provided better performance and lower temperature rise. Next, the full cone nozzle with a medium spray pattern (MPL0.3 M) displayed good cooling performance at higher outlet velocities and flow rates. However, during the hollow cone nozzle L40 operation, no significant variation was seen in the average temperature rise of the hairpin conductor.

The temperature rise distribution on the surfaces of the hairpin conductor against the thermocouples for each nozzle under various conditions is shown in Fig. 7. In the plots, the thermocouples with an odd index monitored the temperature of the top surface of the hairpin conductor and the even ones were used to measure the bottom surface temperature. By comparing the plots, all the thermocouples used to monitor the temperature of the top surface show a slightly lower temperature than thermocouples measuring the bottom side, due to direct contact of the top surface of the hairpin conductor with the spray droplets. Due to the spray flow concentration in the middle of the conductor, thermocouples T3 and T4 showed a lower temperature rise except for hollow cone nozzle L40 (due to the specific spray pattern in the hollow cone format).

Besides, it was observed that the temperature distribution on the rectangular conductor is more uniform, and the cooling performance of

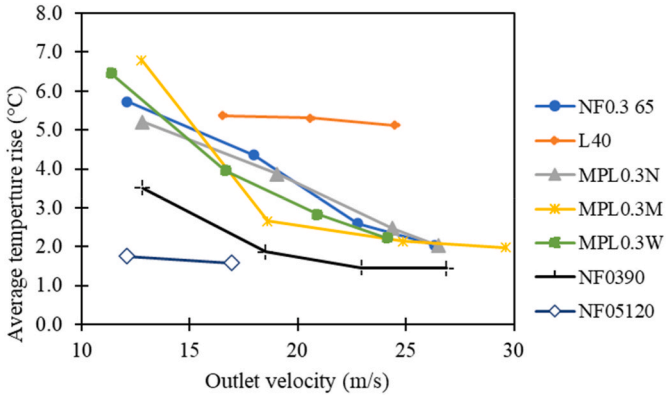

Fig. 6. Variation of the average temperature rise of the rectangular conductor during nozzles' performances versus nozzles' outlet velocity.

Fig. 7. Temperature rise distribution on the surface of the rectangular conductor during the operation of the nozzles under study.

nozzles is improved significantly by increasing the flow rate. Among all the nozzles, the two flat fan nozzles (NF05120 and NF0390) and the full cone nozzle with medium spray angle (MPL0.3 M) provide better temperature uniformity and lower temperature rise.

Ultimately, the nozzles' proper performance in uniform cooling and temperature uniformity are assessed by the standard deviation of the temperature (3). Fig. 8 shows the variation of standard deviation against the nozzles' outlet velocity. The outcomes show that by increasing the outlet velocity, the temperature uniformity was improved due to spraying the oil at a higher flow rate onto the rectangular surface of the hairpin. In addition, the temperature uniformity significantly improved for the hollow cone nozzle at higher outlet velocity. Moreover, the flat fan nozzle NF0390 provided the most stable behavior in uniform cooling and even temperature distribution of the conductor surface.

D. Cooling Efficiency

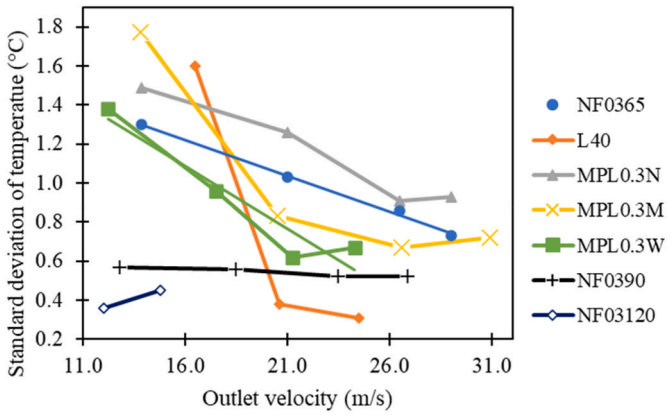

Fig. 8. Variation of the standard deviation of temperature versus nozzles' outlet velocity.

In this section, the efficiency of various nozzle setups is investigated. In the first step, the pumping power and thermal conductance are determined using (4) and (5), respectively. Then, the thermal conductance and the flow rate for each nozzle setup are plotted against the pumping power. Fig. 9 a) and b) show the variation of thermal conductance and flow rate of each nozzle setup versus pumping power, respectively. It was observed that the flat fan nozzle NF05120 provided the highest flow rate and thermal conductance at small pumping power. In the second position again, another flat fan nozzle, NF0390, showed good efficiency by providing a higher flow rate, lower pumping power, and higher thermal conductance. L40 with the hollow cone spray pattern had the weakest efficiency; this nozzle had the lowest flow rate and thermal conductance versus pumping power.

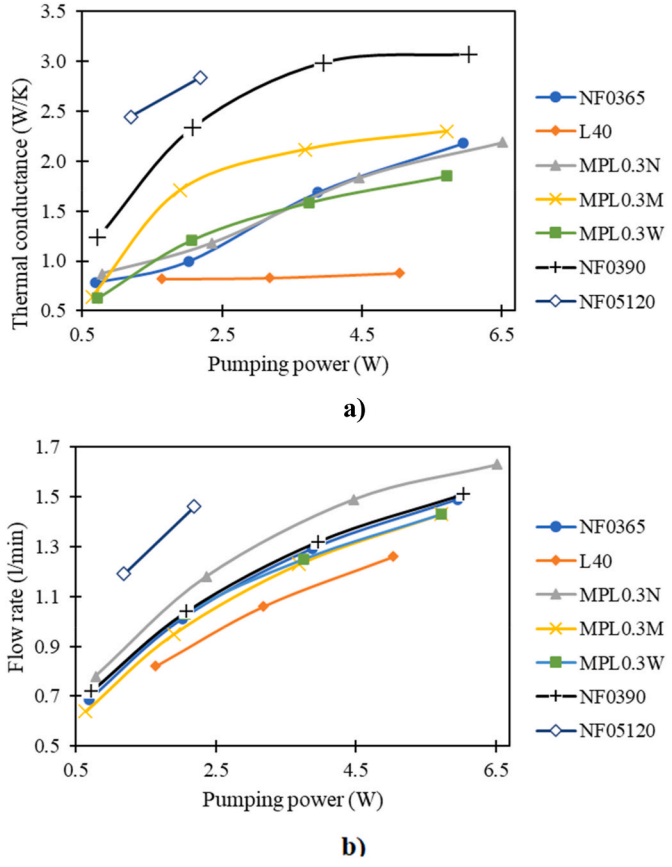

Fig. 9. Investigating the efficiency of nozzle setups. a) Thermal conductance versus pumping power. b) Flow rate against pumping power.

Among the full cone nozzles, MPL0.3 M with medium spray angle showed the greatest thermal conductance. The MPL0.3 N provided a higher flow rate versus almost the same pumping power; however, due to its narrow spray angle, it could not provide high HTC and thermal conductance.

4. Conclusion

This paper experimentally investigates the selection of suitable nozzles for spray cooling systems with high viscosity coolant and the impact of nozzles' inlet pressure and flow rate, spray patterns, and spray angles on the heat transfer capability, cooling and temperature uniformity, and cooling efficiency. The findings from the paper provide valuable insights into the impact of different nozzle parameters, spray patterns, and spray angles on the heat transfer capability, cooling efficiency, and temperature uniformity in a spray cooling system for electric motor components.

A breakdown of the main findings can be summarized as follows:

1. Pressure, flow rate, and outlet velocity**:** Increasing pressure led to higher flow rates and outlet velocities from the nozzles. There was a proportion between pressure and these parameters across all cases studied.
2. Nozzle types and flow rates**:** The flat fan nozzle NF05120 specifically delivered the highest flow rate at the same pressure and exhibited the highest HTC.
3. Effect of flow rate on HTC: Higher flow rates resulted in a significant increase in HTC for all nozzles studied. Flat fan nozzles, especially NF05120, demonstrated the highest HTC, whereas hollow cone nozzles like L40 exhibited the lowest HTC due to lower flow rates.
4. Impact of spray patterns: The spray pattern of the nozzles significantly influenced cooling performance. Flat fan nozzles concentrated fluid in a more targeted manner, providing better operation compared to full cone nozzles, which covered a larger surface area and distributed less fluid. Hollow cone nozzle had the weakest performance due to their spray pattern.
5. Spray angles: Nozzle spray angles also played a crucial role in cooling performance and temperature uniformity. For flat fan nozzles, wider spray angles led to more uniform temperature distribution. NF0390 and NF05120, with medium and wide spray angles, performed better. Among full cone nozzles, MPL0.3 M with a medium spray angle performed better, while MPL0.3 N with a narrow spray angle showed weaker performance.
6. Cooling efficiency: Two flat fan nozzles with medium and wide spray angles exhibited the best cooling efficiency and thermal conductance. The full cone nozzle with a medium spray angle also performed reasonably well, while the hollow cone nozzle L40 showed the weakest cooling efficiency and thermal conductance.

These findings collectively emphasize the importance of nozzle design, flow rates, spray patterns, and spray angles in optimizing cooling performance, temperature uniformity, and cooling efficiency in spray cooling systems for electric motor components. The results provide guidance for selecting appropriate nozzles to enhance the heat transfer capabilities and overall efficiency of such systems.

CRediT authorship contribution statement

Payam Shams Ghahfarokhi: Writing – original draft, Validation, Project administration, Methodology, Investigation, Funding acquisition, Formal analysis, Data curation, Conceptualization. **Andrejs Podgornovs:** Writing – review & editing. **Antonio J. Marques Cardoso:** Writing – review & editing. **Paavo Rasilo:** Writing – review & editing, Visualization, Methodology, Funding acquisition.

Declaration of competing interest

The authors declare that they have no known competing financial interests or personal relationships that could have appeared to influence the work reported in this paper.

Data availability

The authors do not have permission to share data.

References

[1] T.N. Lamichhane, L. Sethuraman, A. Dalagan, H. Wang, J. Keller, M. P. Paranthaman, Additive manufacturing of soft magnets for electrical machines—a review, Materials Today Physics 15 (Dec. 01, 2020) 100255. Elsevier Ltd.

[2] P.S. Ghahfarokhi, et al., Opportunities and challenges of utilizing additive manufacturing approaches in thermal management of electrical machines, IEEE Access 9 (2021) 36368–36381.

[3] S. Nuzzo, D. Barater, C. Gerada, P. Vai, Hairpin windings: an opportunity for next-generation E-motors in transportation, IEEE Industrial Electronics Magazine 16 (4) (Dec. 2022) 52–59.

[4] P. Shams Ghahfarokhi, A. Podgornovs, A.J.M. Cardoso, A. Kallaste, A. Belahcen, T. Vaimann, Hairpin windings for electric vehicle motors: modeling and investigation of AC loss-mitigating approaches, Machines 10 (11) (2022).

[5] N. Bianchi, G. Berardi, Analytical approach to design hairpin windings in high performance electric vehicle motors, in: 2018 IEEE Energy Conversion Congress and Exposition, ECCE 2018, Institute of Electrical and Electronics Engineers Inc., Dec. 2018, pp. 4398–4405.

[6] G. Berardi, N. Bianchi, Design guideline of an AC hairpin winding, in: Proceedings - 2018 23rd International Conference on Electrical Machines, ICEM 2018, Institute of Electrical and Electronics Engineers Inc., Oct. 2018, pp. 2444–2450.

[7] G. Volpe, M. Popescu, F. Marignetti, J. Goss, AC winding losses in automotive traction e-machines: a new hybrid calculation method, in: 2019 IEEE International Electric Machines and Drives Conference, IEMDC 2019, Institute of Electrical and Electronics Engineers Inc., May 2019, pp. 2115–2119.

[8] Y. Zhao, D. Li, T. Pei, R. Qu, Overview of the rectangular wire windings AC electrical machine, CES Transactions on Electrical Machines and Systems 3 (2) (Jun. 2019) 160–169.

[9] C. Liu, et al., Experimental investigation on oil spray cooling with hairpin windings, IEEE Trans. Ind. Electron. 67 (9) (Sep. 2020) 7343–7353.

[10] J.R. Rybicki, I. Mudawar, Single-phase and two-phase cooling characteristics of upward-facing and downward-facing sprays, Int. J. Heat Mass Tran. 49 (1–2) (Jan. 2006) 5–16.

[11] N. Karwa, S.R. Kale, P.M.V. Subbarao, Experimental study of non-boiling heat transfer from a horizontal surface by water sprays, Exp. Therm. Fluid Sci. 32 (2) (Nov. 2007) 571–579.

[12] I. Mudawar, W.S. Valentine, Determination of the local quench curve for spray-cooled metallic surfaces, J. Heat Treat. 7 (2) (Sep. 1989) 107–121.

[13] S.S. Hsieh, C.H. Tien, R-134a spray dynamics and impingement cooling in the non-boiling regime, Int. J. Heat Mass Tran. 50 (3–4) (Feb. 2007) 502–512.

[14] D.J. Womac, S. Ramadhyani, F.P. Incropera, Correlating equations for impingement cooling of small heat sources with single circular liquid jets, J. Heat Tran. 115 (1) (Feb. 1993) 106–115.

[15] X. Liu, et al., The suppression of thermal propagation using spray cooling with R410A in overheated lithium battery pack, Case Stud. Therm. Eng. 58 (Jun. 2024) 104339.

[16] X. Chen, et al., Heat transfer of single-phase spray cooling on heated vibrating surfaces, Case Stud. Therm. Eng. 50 (Oct. 2023) 103489.

[17] C. Liu, et al., Estimation of oil spray cooling heat transfer coefficients on hairpin windings with reduced-parameter models, IEEE Transactions on Transportation Electrification 7 (2) (2021) 793–803. June 2021(Oct. 2020).

[18] Y.C. Chong, et al., Experimental characterisation of radial oil spray cooling on a stator with hairpin windings, in: IET Conference Publications, Institution of Engineering and Technology, 2020, pp. 879–884.

[19] F. Zhang, et al., A thermal modeling approach and experimental validation for an oil spray-cooled hairpin winding machine, IEEE Transactions on Transportation Electrification 7 (4) (Dec. 2021) 2914–2926.

[20] P.O. Gronwald, N. Wiese, T.A. Kern, M. Henke, Electric traction motor spray cooling - empirical model development and experimental validation, IEEE Transactions on Transportation Electrification 9 (2) (Jun. 2023) 2185–2194.

[21] P.S. Ghahfarokhi, A. Podgornovs, A. Kallaste, A.J.M. Cardoso, A. Belahcen, T. Vaimann, The oil spray cooling system of automotive traction motors: the state of the art, IEEE Transactions on Transportation Electrification 9 (1) (2023) 428–451.

[22] P.S. Ghahfarokhi, et al., Experimental investigation of high viscosity on oil spray cooling system with hairpin winding, 2023 IEEE 14th International Symposium on Diagnostics for Electrical Machines, Power Electronics and Drives (SDEMPED) (Aug. 2023) 234–238.

[23] G. Liang, I. Mudawar, Review of spray cooling – Part 1: single-phase and nucleate boiling regimes, and critical heat flux, Int. J. Heat Mass Tran. 115 (Dec. 01, 2017) 1174–1205. Elsevier Ltd.

[24] R.J. Schick, Spray Technology Reference Guide: Understanding Drop Size Preface, 47th Chemical Processing Industry Exposition, 1997, p. 6.